

TCSC Controller Design for Damping Interarea Oscillations

Ning Yang Qinghua Liu James D. McCalley
yangning@iastate.edu *qxll1@pge.com* *jdm@iastate.edu*
 Student Member Student Member Senior Member
 Iowa State University
 Ames Iowa

Abstract— Thyristor Controlled Series Compensator (TCSC), a prominent FACTS device, can rapidly modulate the impedance of a transmission line, resulting in improvement of system performance. The purpose of the work reported in this paper is to design a controller to damp interarea oscillations. We have applied the residue method to the linearized power system equations and obtained a generalized form which is suitable for different controller input/output channels and therefore suitable for different control devices. This method, together with modal sensitivities, is applied to TCSC to determine the location, feedback signal, and controller design. The damping result is illustrated by comparing changes in damping ratio and identifying the increase of transfer capacity.

Keywords— TCSC, control, interarea oscillations, eigenvalues, residue, transmission

I. INTRODUCTION

Damping of electro-mechanical oscillation between interconnected synchronous generators is necessary for secure system operation. A large power system has numerous modes of oscillation. These modes can be placed into two categories, local modes and interarea modes. Interarea modes are more difficult to analyze and damp, since they are influenced by global states, and therefore their analysis requires the detail of the interconnected system.

FACTS devices are capable of improving steady state and dynamic system performance. Since system oscillations are heavily influenced by line impedance, TCSC can be very effective in providing additional damping.

Different control methods and signals [1], [2] have been applied to TCSC to damp system oscillations. The method presented in this paper is based on modal sensitivity and on functional sensitivity [3] from small signal stability analysis. The functional sensitivity, or residue method performs eigenvalue placement using the residue. It was applied to PSS in [4], [5], [6].

PE-122-PWRS-0-12-1997 A paper recommended and approved by the IEEE Power System Dynamic Performance Committee of the IEEE Power Engineering Society for publication in the IEEE Transactions on Power Systems. Manuscript submitted June 3, 1997; made available for printing December 12, 1997.

When we apply this method to various FACTS devices such as TCSC or SVC, some issues have to be addressed. First, since there are several possible input/output pairs, it would be helpful to obtain a model for control design that is applicable to all of them. Reference [2] provides one. This paper provides another one which is attractive because of its compact matrix representation. Second, in the case of TCSC, since it can be considered as the combination of steady state compensation and a small deviation of compensation in the small signal stability analysis, simply calculating the functional sensitivity as in [7], does not account for the influence of the TCSC steady state compensation.

In section II, we briefly review the basics of using residue for control design. Section III provides a unified model of power system control design that can be used for various types of control devices at any location. Section IV applies the model of section III to TCSC installation in a sample system that has been previously used in the literature. Conclusions are made in section V.

II. THE RESIDUE METHOD

A. Functional sensitivity

Figure 1 shows the transfer function of the closed-loop system, where:

$$G(s) = C(sI - A)^{-1}B + D \quad (1)$$

is the transfer function of original system, and $KH(s)$ is the transfer function of the controller. K is a constant gain.

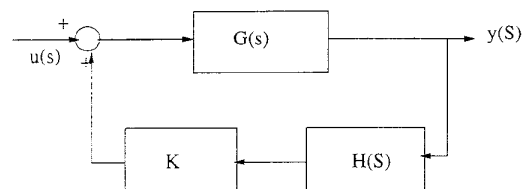


Fig. 1. Transfer Function

The transfer function between the k th input and the j th output $G_{jk}(s)$ can be expressed in terms of residues and system eigenvalues as:

$$G_{jk}(s) = \sum_{i=1}^n \frac{R_{ijk}}{(s - \lambda_i)} \quad (2)$$

where R_{ijk} is the residue associated with i th mode, k th output and j th input. R_{ijk} can be expressed as:

$$R_{ijk} = C_j t_i v_i B_k \quad (3)$$

where t_i and v_i denote the right and left eigenvectors, respectively associated with the i th eigenvalue.

Additionally, the residue can be expressed in terms of mode controllability and observability. The controllability of mode i from the j th input is given by:

$$cont_{ij} = |v_i B_j| \quad (4)$$

The measure of mode observability of mode i from output k is given by:

$$obs_{ik} = |C_k t_i| \quad (5)$$

It is clear that

$$|R_{ijk}| = |C_k t_i v_i B_j| = obs_{ik} \cdot cont_{ij} \quad (6)$$

Reference [3] shows that the residue associated with an eigenvalue λ_i and a feedback transfer function $\phi(s, K)$, where K is constant gain of the controller, are related by:

$$\frac{\partial \lambda_i}{\partial K} = R_{ijk} \frac{\partial \phi(s, K)}{\partial K} \quad (7)$$

Eqt. 7 is known as functional sensitivity [4]. It gives the relation between the sensitivity of eigenvalue to feedback loop gain and the open loop residue associated with the same eigenvalue.

The feedback transfer function in Figure 1 is:

$$\phi(s, K) = KH(s) \quad (8)$$

Substitution of $\phi(s, K)$ into eqt. 7, and assuming the gain K is small, we have:

$$\frac{\Delta \lambda_i}{\Delta K} = R_{ijk} H(\lambda_i) \quad (9)$$

If $K = 0$ in the initial operating point, ΔK is equal to K . Therefore, adding the feedback to the system will cause a change in i th eigenvalue as:

$$\Delta \lambda_i = R_{ijk} KH(\lambda_i) \quad (10)$$

B. Control Design Approach

Eqt. 10 shows the relation between the change in the i th eigenvalue and residue associated with the i th eigenvalue. For each oscillatory mode, λ_i has a complex conjugate, and so does the corresponding residue. We can design a lead/lag compensation controller to shift the residue to the negative axis, as shown in Figure 2, so as to make the real component of $\Delta \lambda_i$ more negative. The form of the compensator design is given in [6] as:

$$KH(s) = K \frac{sT}{1+sT} \left[\frac{1+sT_1}{1+sT_2} \right]^m \quad (11)$$

where:

$$\begin{aligned} \phi &= 180^\circ - \arg(R_{ijk}) \\ \alpha &= \frac{T_2}{T_1} = \frac{1 - \sin(\frac{\phi}{m})}{1 + \sin(\frac{\phi}{m})} \\ T_1 &= \frac{1}{\omega_i \sqrt{\alpha}} \\ T_2 &= \alpha T_1 \end{aligned}$$

T is the washout time constant (usually 5-10 sec.), ω_i is the frequency of the poorly damped mode in rad/sec, K is a positive constant gain, and m is the number of compensation stages. The angle compensated by each block should not exceed 60° .

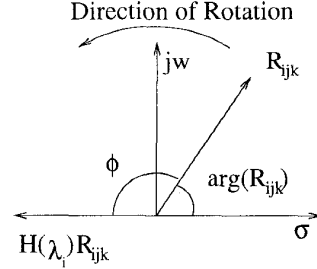


Fig. 2. Concept of compensation

III. GENERAL APPLICATION IN POWER SYSTEM

In this section we provide an approach for controller design that is generalized in that it can be used for various types of control device, at any location, by specifying only the controller input and output signal. We assume in this approach that the controller can be modeled in the form given in eqt. 11.

A. System Modes

The equations to describe the oscillatory behavior of a power system are composed of a mix of differential and algebraic equations that can be expressed as:

$$\begin{aligned} \dot{X}_1 &= f(X_1, X_2, u) \\ 0 &= g(X_1, X_2, u) \end{aligned} \quad (12)$$

where X_1 denotes system state variables, X_2 denotes voltage magnitudes and angles, and u is an output signal for any specific controller of interest. We define Y as the controller input so that:

$$Y = h(X_1, X_2, u) \quad (13)$$

By linearization, we obtain:

$$\begin{aligned} \Delta \dot{X} &= A \Delta X + B \Delta u \\ \Delta Y &= C \Delta X + D \Delta u \end{aligned} \quad (14)$$

where $\Delta X = \Delta X_1$ is the vector of state variables.

Eigen analysis of the system A-matrix will produce system eigenvalues λ_i and their corresponding right and left eigenvectors t_i, v_i , respectively. Some of the modes are defined as local modes and others are interarea modes as indicated by the frequency range and system states by which the modes are affected. The aim of the design of the controller is to increase the damping of the poorly damped interarea modes.

B. Influence of controller output signal

From the concept of residue we know that the controller output signal (i.e., the input signal of the original system) directly affects the controllability and the corresponding residue. Different power system control devices have different output signals. As for PSS, the output of the controller is mixed with V_{ref} as an AVR input; for some of the FACTS devices, the output may be the thyristor firing angle. Representing the controller output signal as u , the linearization of eqt. 12 results:

$$\begin{aligned}\Delta \dot{X}_1 &= \frac{\partial f}{\partial X_1} \Delta X_1 + \frac{\partial f}{\partial X_2} \Delta X_2 + \frac{\partial f}{\partial u} \Delta u \\ 0 &= \frac{\partial g}{\partial X_1} \Delta X_1 + \frac{\partial g}{\partial X_2} \Delta X_2 + \frac{\partial g}{\partial u} \Delta u\end{aligned}\quad (15)$$

Some manipulation yields:

$$\Delta X_2 = -\frac{\partial g}{\partial X_2}^{-1} \left[\frac{\partial g}{\partial X_1} \Delta X_1 + \frac{\partial g}{\partial u} \Delta u \right] \quad (16)$$

$$\begin{aligned}\Delta \dot{X}_1 &= \left[\frac{\partial f}{\partial X_1} - \frac{\partial f}{\partial X_2} \frac{\partial g}{\partial X_2}^{-1} \frac{\partial g}{\partial X_1} \right] \Delta X_1 \\ &+ \left[\frac{\partial f}{\partial u} - \frac{\partial f}{\partial X_2} \frac{\partial g}{\partial X_2}^{-1} \frac{\partial g}{\partial u} \right] \Delta u\end{aligned}\quad (17)$$

Comparison of eqt. 16 to eqt. 14 indicates that the matrix A and vector B in eqt. 14 are:

$$A = \frac{\partial f}{\partial X_1} - \frac{\partial f}{\partial X_2} \frac{\partial g}{\partial X_2}^{-1} \frac{\partial g}{\partial X_1} \quad (18)$$

$$B = \frac{\partial f}{\partial u} - \frac{\partial f}{\partial X_2} \frac{\partial g}{\partial X_2}^{-1} \frac{\partial g}{\partial u} \quad (19)$$

Eqt. 18 and 19 show that the choice of controller output signal u only affects the B vector, and it has no influence on the A matrix.

C. Influence of controller input signal

The controller input signal is related to the residue via the observability. Generator frequency deviation, bus voltage and real power flow are all good candidates for controller local input signals. If one is willing to accept additional expense associated with communication, global signals such as intermachine speed difference may be used. Representing these kinds of signals, global or local, as y , the linearization of the output signal in eqt. 14 yields:

$$\Delta y = \frac{\partial h}{\partial X_1} \Delta X_1 + \frac{\partial h}{\partial X_2} \Delta X_2 + \frac{\partial h}{\partial u} \Delta u \quad (20)$$

Substitution of eqt. 16 results in:

$$\begin{aligned}\Delta y &= \left[\frac{\partial h}{\partial X_1} - \frac{\partial h}{\partial X_2} \frac{\partial g}{\partial X_2}^{-1} \frac{\partial g}{\partial X_1} \right] \Delta X_1 \\ &+ \left[\frac{\partial h}{\partial u} - \frac{\partial h}{\partial X_2} \frac{\partial g}{\partial X_2}^{-1} \frac{\partial g}{\partial u} \right] \Delta u\end{aligned}\quad (21)$$

Comparison to eqt 14 indicates that:

$$C = \frac{\partial h}{\partial X_1} - \frac{\partial h}{\partial X_2} \frac{\partial g}{\partial X_2}^{-1} \frac{\partial g}{\partial X_1} \quad (22)$$

$$D = \frac{\partial h}{\partial u} - \frac{\partial h}{\partial X_2} \frac{\partial g}{\partial X_2}^{-1} \frac{\partial g}{\partial u} \quad (23)$$

Therefore, different controller input signals result in different C and D vectors.

D. Determination of controller parameters

The controller gain K is computed as a function of the desired eigenvalue location $\lambda_{i,des}$ according to eqt. 10 so that:

$$K = \frac{\lambda_{i,des} - \lambda_i}{R_{ijk} H(\lambda_i)} \quad (24)$$

where we assume that the phase compensation of $H(\lambda_i)$ provides that K is real. Since eqt. 10 is derived under the assumption that K is small, the eigenvalue after the controller design may be different from the desired one. Moreover we need to check that the influence of the controller on the other modes is acceptable. If not, or under the condition that we desire to damp more than one mode, we may replace R_{ijk} in eqt. 11 and eqt. 24 with a weighted summation of the residue for all modes that are to be damped, such that the least stable modes have greater weight than the more stable modes. This approach for damping multiple modes may require several iterations.

E. Location problem

From eqt. 10, it is easy to see that for the same gain of the feedback loop, a larger residue will result in a larger change in the corresponding mode. Therefore the best input and output of the controller are those which give the largest residue for the desired mode.

One practical consideration in choosing the input/output pair is the cost of the compensator. Therefore, high residue input/output pairs that require more than 60° phase shift may be less desirable than the lower residue pairs that require less than 60° of phase shift, since 60° is an approximate phase limit for each compensator stage.

IV. APPLICATION TO TCSC

A. Calculation of system matrix of controller output

The design method mentioned above is suitable for application to various controllers. Here, we apply it to TCSC. We assume that the impedance associated with the TCSC is:

$$Z_{TCSC} = Z_{TCSC}^{(0)} + \Delta Z_{TCSC}(s) \quad (25)$$

$$\Delta Z_{TCSC}(s) = \frac{\Delta Z_{TCSC}}{1 + sT_{TCSC}} \quad (26)$$

where $Z_{TCSC}^{(0)}$ is the steady state impedance of the device and $\Delta Z_{TCSC}(s)$ represents the control influence on the

TCSC impedance. T_{TCSC} is the time constant of TCSC which is 0.015s, and ΔZ is the desired compensation of the controller [8]. So the line impedance after installation of TCSC is:

$$Z_{line} = Z_{line}^{(0)} - Z_{TCSC} \quad (27)$$

where $Z_{line}^{(0)}$ is the line reactance in steady state. Since the reactance of the line is constant, the change in total line reactance is:

$$\Delta Z_{line} = -\Delta Z_{TCSC}(s) \quad (28)$$

Hence we can take the change of impedance of a transmission line as the output of the controller. By substituting Z_{line} for u in eqt. 19, the B matrix can be calculated. The TCSC control loop is shown in Fig. 3.

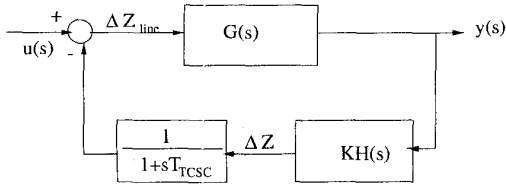


Fig. 3. Controller Loop of TCSC

B. Influence of different controller input

TCSC is more effective in damping interarea oscillations when the controller input is a global signal. We have found that the speed difference of two generators which oscillate against each other gives a large observability, and so does the change in tie line real power flow. So either of these signals can serve as the input to TCSC controller.

Using speed difference as the controller input signal, since the changes of speed are state variables, the output Y can be expressed as:

$$\Delta Y = a \Delta X_1 \quad (29)$$

where: $a = [0, 0, \dots, 0, 1, \dots, -1, 0, \dots, 0]$ and 1 and -1 in the a vector corresponds to the speed difference as $\Delta \omega_i - \Delta \omega_j$. Therefore from eqt. 22 the C and D matrices are: $C = a$ and $D = 0$.

Interarea modes typically have high observability in the active power of tie lines between areas involved in the interarea oscillation and high controllability in the susceptance of the same line. So it is efficient and practical to install TCSC in a tie line and use the line active power flow as the controller input.

The tie line active power flow is a function of voltage magnitude and angle, which comprise X_2 . Therefore we may write:

$$P = h(X_2) \quad (30)$$

By setting $\frac{\partial h}{\partial X_1} = 0$ in eqt. 22, C and D can be easily computed.

C. Determination of Location

Because TCSC consists of a steady state, fixed value of compensation together with control capability, identification of the most effective TCSC location, in the most general case, must be solved in two separate steps. In step 1, we identify the most effective location with respect to steady state issues. These issues may include the effect on small signal stability, voltage control and stability, subsynchronous resonance, flow control, and others. In this paper, we limit our consideration to the effect on small signal stability, and we assess this effect using modal sensitivity, as described in subsection C.1 below. Once we identify one or more possible locations for installation at fixed compensation, then we proceed to step 2, where we identify from among them the best possible control location. In this step, we use the functional sensitivity approach, as described in subsection C.2 below, where each location and consequently each input/output pair is analyzed with the fixed compensation installed for that location.

C.1 Step 1

The system in eqt. 12 can be expressed in the form of eqt. 31,

$$B_e \dot{X}_e = A_e X_e \quad (31)$$

where B_e is a diagonal matrix with entry '1' for differential equations and entry '0' for algebraic equations, X_e includes both X_1 and X_2 , and A_e is the corresponding coefficients matrix.

Let ϕ_i and ψ_i denote the right and left eigenvectors corresponding to the generalized eigenvalue problem. The eigenvectors can be chosen so that the following conditions are satisfied for each eigenvalue.

$$A_e \phi_i = \lambda_i B_e \phi_i \quad (32)$$

$$\psi_i A_e = \lambda_i \psi_i B_e \quad (33)$$

$$\psi_i B_e \phi_i = 1 \quad (34)$$

Using the formulation in [9], the sensitivity with respect to line susceptance B_l is:

$$\frac{\partial \lambda_i}{\partial B_l} = \frac{\psi_i \frac{\partial A_e}{\partial B_l} \phi_i - \lambda_i \psi_i \frac{\partial B_e}{\partial B_l} \phi_i}{\psi_i B_e \phi_i} \quad (35)$$

and with $\frac{\partial B}{\partial B_l} = 0$,

$$\frac{\partial \lambda_i}{\partial B_l} = \frac{\psi_i \frac{\partial A_e}{\partial B_l} \phi_i}{\psi_i B_e \phi_i} \quad (36)$$

We see from equation 36 that we may obtain $\frac{\partial \lambda_i}{\partial B_l}$ if we can compute $\frac{\partial A_e}{\partial B_l}$. To this end, we note that state variables,

voltage magnitudes and phase angles are all dependent on the line parameter B_l , i.e.,

$$\begin{aligned} x_1 &= h_1(B_l) \\ x_2 &= h_2(B_l) \end{aligned} \quad (37)$$

Therefore, by the chain rule for partial differentiation,

$$\begin{aligned} \frac{\partial A_e}{\partial B_l} &= \frac{\partial A_e}{\partial B_l} \Big|_{B_{10}, x_{10}, x_{20}} + \frac{\partial A_e}{\partial x_1} \Big|_{B_{10}, x_{10}, x_{20}} \frac{\partial x_1}{\partial B_l} \\ &+ \frac{\partial A_e}{\partial x_2} \Big|_{B_{10}, x_{10}, x_{20}} \frac{\partial x_2}{\partial B_l} \end{aligned} \quad (38)$$

The partial derivatives $\partial x_1/\partial B_l$ and $\partial x_2/\partial B_l$ in eqt. 38 are regarded as indirect sensitivities and are obtained at the equilibrium point of the system, i.e., for a given operating condition, as denoted by x_{10} , x_{20} and B_{10} .

The equilibrium point of the system can be expressed from equations 12 as:

$$\begin{aligned} 0 &= f(x_1, x_2, B_l) \\ 0 &= g(x_1, x_2, B_l) \end{aligned} \quad (39)$$

Taking the partial derivative with respect to B_l for both equations, we obtain:

$$\frac{\partial f}{\partial B_l} = A_{11} \frac{\partial x_1}{\partial B_l} + A_{12} \frac{\partial x_2}{\partial B_l} \quad (40)$$

$$\frac{\partial g}{\partial B_l} = A_{21} \frac{\partial x_1}{\partial B_l} + A_{22} \frac{\partial x_2}{\partial B_l} \quad (41)$$

so that:

$$\begin{bmatrix} A_{11} & A_{12} \\ A_{21} & A_{22} \end{bmatrix} \begin{bmatrix} \frac{\partial x_1}{\partial B_l} \\ \frac{\partial x_2}{\partial B_l} \end{bmatrix} = \begin{bmatrix} \frac{\partial f}{\partial B_l} \\ \frac{\partial g}{\partial B_l} \end{bmatrix} \quad (42)$$

We use LU factorization to get the left-hand side of equation 42.

C.2 Step 2

In order to compare the residues associated with different input and output signals, we form the \hat{B} and \hat{C} matrices. These two matrices are related to the B and C vector in eqt. 19 and eqt. 22. The k th column of the \hat{B} matrix is a specific B vector and denotes the influence of change in susceptance of the k th line on the system state. The j th row in the \hat{C} matrix is a specific C vector and represents one possible combination of speed difference when the input to the controller is the speed difference signal; for the input of tie line flow, the j th row represents the line number from which the power flow signal comes. Then, the residue matrix can be calculated as:

$$R_i = \hat{C}_i v_i \hat{B} \quad (43)$$

The k and j associated with the location in R_i of the largest residue gives the best location and controller input signal.

If the controller uses only local measurements, the input and output are associated with the same circuit. Therefore, consideration of local signals requires that we choose the largest element on the diagonal of the residue matrix in eqt. 43.

Note that the line associated with the largest residue for speed difference input signal may not be the same as the line associated with the largest residue for tie line flow input signal. This is because for each line the observability factor for speed difference is not the same as the observability factor for tie line flow. In addition, we note that when using a speed difference input signal, since there is no local measurement of such a signal, we choose the machine speed differences that give the largest observability, and we use the same speed difference signal for all lines considered as potential locations. Therefore in the case of speed difference signal, the observability factor is the same for all candidate locations, and the TCSC effectiveness depends only on controllability. On the other hand, when using the tie line real power flow as TCSC input, a local measurement, the input is unique to each candidate location, and the effectiveness depends on both controllability and observability of the same line.

D. Numerical Example

A 3-area, 6-machine sample system [10] presented in Figure 4 is used to illustrate the siting and control approach. This system gives 3 local modes and 2 interarea modes. Although this is a test system, it well serves to illustrate the approach, which remains the same for large systems. The upper line between 10-11 is an equivalent line [10] (which has impedance smaller than the lower one) and therefore not a candidate for compensation. These two lines serve as a tie line that connects area A with the others. Stressing the system by increasing the load at bus #10 and generation at bus #6, one interarea oscillatory mode becomes unstable, as indicated in Table I.

TABLE I
Interarea modes before static compensation

Real Load at Bus #10		100 MW	500 MW
Mode 1	f (Hz)	0.8774	0.8157
	ξ %	1.6896	-1.5741
Mode 2	f (Hz)	1.1236	1.0841
	ξ %	8.0260	7.5929

We compute the modal sensitivities for the unstable mode to the line susceptance and list in Table II in rank order the most effective lines. Since line #10 to #11 has the largest sensitivity, it is a good candidate to install TCSC. This line is compensated to 40 %. After this compensation, one

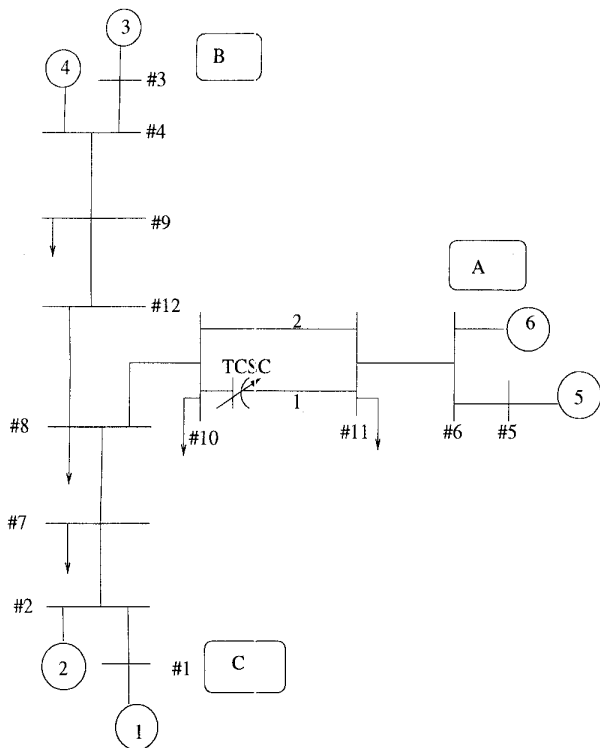


Fig. 4. Sample System

TABLE II
Modal sensitivities to line susceptance

Rank	Line	Value
1	10 - 11(1)	0.1142
2	9 - 12	0.0713
3	6 - 11	0.0107
4	4 - 9	0.0071
5	8 - 10	0.0044

mode is still unstable as in Table III. The mode shape of the unstable mode is shown in Figure 5. It clearly shows that the group of generators 3 and 4 oscillate against the group of generators 5 and 6.

In Table V, we compare the residue of the two interarea modes for the input/output pairs of Table IV. The phase of mode 1 and 2 are close for each controller input; also it is shown in Table III that the frequency of these two interarea modes are close to each other. Therefore, a controller designed using either of these two modes will also improve the other. Since mode 1 is unstable, we will use the residue and frequency of mode 1 for the controller design.

Setting the desired damping ratio ξ for mode 1 as 20 %, we use eqt. 24 to calculate the gain K . The two interarea modes are shown in Table VI, where the load at bus #10 is 500 MW. For the same mode 1 damping ratio, the controller using tie line flow signal has smaller feedback gain. The difference between desired and calculated damping ratio is due to the fact eqt. 10 is exact only for very small

TABLE III
Interarea modes after static compensation

Real Load at Bus #10		500 MW
Mode 1	$f(\text{Hz})$	0.8882
	$\xi\%$	-0.2475
Mode 2	$f(\text{Hz})$	1.1349
	$\xi\%$	6.8664

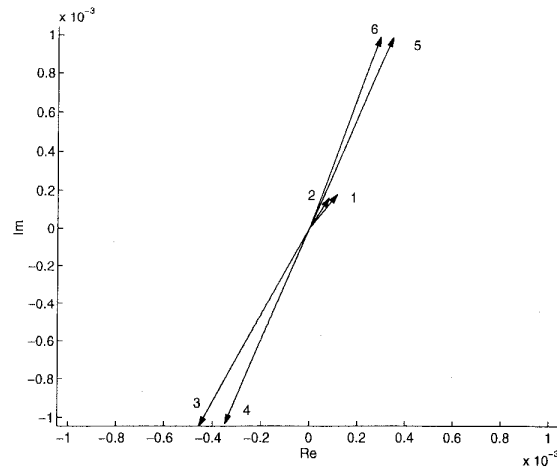


Fig. 5. Mode Shape of Mode 1

feedback gain, which we verified through calculation. In addition, we observe that the other interarea mode (mode 2) has not been degraded significantly by either controller, our result (not shown) also indicates no significant degradation occurs in the local modes as well.

The performance of the controller can also be shown in terms of the increase of transfer capacity. Without TCSC, the maximum load at bus #10 is 400 MW. When TCSC with controller using difference of speed deviation input is installed, the maximum load is 550 MW. When TCSC with controller using line active power input is installed, the maximum load is 800 MW, which is twice that of the load without TCSC. Therefore, the TCSC controller yields an expanded secure operating region, and we find that use of tie line flow input signal is more effective than use of speed difference input signal.

V. CONCLUSIONS

This paper presents a unified model for various input/output pairs in the power system. Application of modal and functional sensitivity to this model provides that we can locate and design different kinds of power system controllers. The method is illustrated by applying it to TCSC controller design for damping interarea oscillations. A two step procedure is developed identifying the most effective location for fixed and controlled compensation. A numerical example illustrates the effectiveness of

TABLE IV
Residues of Different Controller Input

	Speed diff.	Tie line flow
$Residue_{max}$	0.1537	0.3342
Input Signal	$\Delta\omega_4 - \Delta\omega_6$	$\Delta P_{tie10-11}$
Location	Line 10-11	Line 10-11

TABLE V
Residues of Two Interarea Modes

	Speed diff.		Tie line flow	
	Mode1	Mode2	Mode1	Mode2
Residue	0.1537	0.0286	0.3342	0.3342
Phase(Residue)	20.258	51.129	89.756	67.771

TCSC damping performance. Also it shows that for this test system, the tie line flow signal is more effective than speed difference signal as the input of TCSC. Use of tie line flow rather than speed difference as TCSC input signal is attractive since it is based on local measurements only.

ACKNOWLEDGMENTS

The support of NSF grant ECS9309092 is gratefully acknowledged.

REFERENCES

- [1] P.S. Dolan, J.R. Smith, and W.A. Mittelstadt, "Study of TCSC optimal damping control parameters for different operating conditions," *IEEE Transactions on Power System*, vol. 10, no. 4, pp. 1972-1978, November 1995.
- [2] H.F. Wang and F.J. Swift, "A unified model for analysis of FACTS devices in damping power system oscillations part I: Single-machine infinite-bus power systems," *IEEE Transactions on Power Delivery*, vol. 12, no. 2, pp. 941-946, April 1997.
- [3] F.Luis Pagola, Ignacio J. Perez-Arriaga and George C. Verghese, "On sensitivities, residues and participations: applications to oscillatory stability analysis and control," *IEEE Transactions on Power Systems*, vol. 4, no. 1, pp. 278-285, February 1989.
- [4] E.Z. Zhou, "Functional sensitivity concept and its application to power system," *IEEE Transactions on Power Systems*, vol. 9, no. 1, pp. 518-524, February 1994.
- [5] N. Martins, "Oscillation damping analysis and control studies of the future interconnection between the north-northeast and south-southeast systems," V Symposium of Specialists in Electric Operational and Expansion Planning, May, 1996.
- [6] M.E. Aboul-Ela, A.A. Sallam, J. D. McCalley, A.A. Fouad, "Damping controller design for power system oscillation using global signals," *IEEE Transactions on Power System*, vol. 11, no. 2, pp. 767-773, May 1996.
- [7] H.F. Wang and F.J. Swift, M.Li, "Indices for selecting the best location of PSSs or FACTS-based stabilizer in multimachine power system: A comparative study," *IEE Proc. of Generation, Transmission and Distribution*, pp. 155-159, March 1997.
- [8] E. Larsen, C. Bowler, B. Damsky, and S. Nilsson, "Benefits of thyristor controlled series compensation," CIGRE 1992 joint section 14/37/38, Paris, August, 1992.
- [9] Thomas Smed, "Feasible eigenvalue sensitivity for large power systems," *IEEE Transaction on Power Systems*, vol. 8, no. 2, pp. 555-561, May 1993.
- [10] G. N. Taranto, J. H. Chow, H. A. Othman, "Robust decentralized control design for damping power system oscillation," *Proceeding of IEEE 33rd Conference on Decision and Control*, pp. 4080-4085, December 1994, Lake Buena, FL.

TABLE VI
Damped Modes

Feedback loop gain $K \times H(\lambda_i) $	Speed diff.		Tie line flow	
	7.3343		3.4646	
	$f(Hz)$	$\xi\%$	$f(Hz)$	$\xi\%$
Mode 1	0.8224	19.9201	0.8593	45.169
Mode 2	1.1027	9.7090	0.9688	9.1942

BIOGRAPHIES

Ning Yang received his BSEE from Tsinghua University, Beijing, China 1995. He became a project engineer in Beijing HITACHI-HUASUN System Control Corp., Beijing, China in the same year. He has been studying for his MSEE in Iowa State University since 1996. His major area is controller design of FACTS devices.

Qinghua Liu received her B.S. in Electrical Engineering (1993) from Tsinghua University, China. She was a research engineer in Tsinghua University from 1993 to 1995. She came to Iowa State University in Aug. 1995 and obtained her M.S. in May 1997. She is now working for Pacific Gas and Electric Company.

James D. McCalley is Assistant Professor of Electrical and Computer Engineering Department at Iowa State University, where he has been employed since 1992. He worked for Pacific Gas and Electric Company from 1986 to 1990. Dr. McCalley received the B.S. (1982), M.S. (1986), and Ph.D (1992) degrees in Electrical Engineering from Georgia Tech. He is a registered professional engineer in California and a member of the IEEE.